Surv Geophys (2014) 35:431–448
DOI 10.1007/s10712-013-9258-7

Evaluation of Gravity and Aeromagnetic Anomalies for the Deep Structure and Possibility of Hydrocarbon Potential of the Region Surrounding Lake Van, Eastern Anatolia, Turkey

Attila Aydemir · Abdullah Ates · Funda Bilim · Aydin Buyuksarac · Ozcan Bektas

Received: 24 November 2012 / Accepted: 17 October 2013 / Published online: 9 November 2013

Abstract The North Anatolian Fault (NAF) is not observed on the surface beyond 40 km southeast of Karliova town toward the western shoreline of Lake Van. Various amplitudes of gravity and aeromagnetic anomalies are observed around the lake and surrounding region. In the gravity anomaly map, contour intensity is observed from the north of Mus city center toward Lake Van. There is a possibility that the NAF extends from here to the lake. Because there is no gravity data within the lake, the extension of the NAF is unknown and uncertain in the lake and to the east. Meanwhile, it is observed from the aeromagnetic anomalies that there are several positive and negative amplitude anomalies aligned around a slightly curved line in the east–west direction. The same curvature becomes much clearer in the analytic signal transformation map. The volcanic mountains of Nemrut and Suphan, and magnetic anomalies to the east of the Lake Van are all lined up and extended with this slightly curved line, provoking thoughts that a fault zone that was not previously mapped may exist. The epicenter of the major earthquake event that occurred on October 23, 2011 is located on this fault zone. The fault plane solution of this earthquake indicates a thrust fault in the east–west direction, consistent with the results of this study. Volcanic mountains in this zone are accepted as still being active because of gas seepages from their calderas, and magnetic anomalies are caused by buried causative bodies, probably

A. Aydemir (✉)
Turkiye Petrolleri A.O., Sogutozu Mah. 2180. Cad. No: 86, 06100 Sogutozu, Ankara, Turkey
e-mail: aydemir@tpao.gov.tr

A. Ates
Department of Geophysical Engineering, Engineering Faculty, Ankara University, Besevler, Ankara 06100, Turkey

F. Bilim · O. Bektas
Department of Geophysical Engineering, Engineering Faculty, Cumhuriyet University, 58140 Sivas, Turkey

A. Buyuksarac
Department of Geophysical Engineering, Engineering Faculty, Canakkale Onsekiz Mart University, Canakkale, Turkey

magmatic intrusions. Because of its magmatic nature, this zone could be a good prospect for geothermal energy exploration. In this study, the basement of the Van Basin was also modelled three-dimensionally (3D) in order to investigate its hydrocarbon potential, because the first oil production in Anatolia was recorded around the Kurzot village in this basin. According to the 3D modelling results, the basin is composed of three different depressions aligned in the N–S direction and many prospective structures were observed between and around these depressions where the depocenter depths may reach down to 10 km.

Keywords Lake Van · Eastern Anatolia · Nemrut and Suphan mountains · Upward continuation · Vertical derivative · Analytic signal · 3D modelling

1 Introduction

The study area is located in the east of Turkey along the border between Turkey and Iran. The Van Basin is observed to the east of Lake Van, which is the largest lake in Turkey while the Mus Basin lies to the northwest of the lake. Both basins are classified under the intermountain basins of the Eastern Anatolia. Van, Bitlis, and Mus are the largest cities in the study area (Fig. 1). There are numerous studies to investigate the stratigraphy, tectonic setting, seismotectonic structure, magmatism, and hydrocarbon (HC) potential of this area in the literature.

Kurtman and Akkus (1971) studied all sedimentary basins in East Anatolia and their hydrocarbon (HC) potential. Sengor and Kidd (1979) studied the post-collision tectonics in Eastern Anatolia and Iran and compared this region to Tibet. Sengor and Yilmaz (1981) evaluated the Eastern Anatolian high plateau as an accretionary prism. Jackson and McKenzie (1984) studied the active tectonics on the Alpine–Himalayan Belt crossing the study area as far as Pakistan. Saroglu and Yilmaz (1986) investigated the geological evolution of Eastern Anatolia and the basin models. Yilmaz et al. (1987) studied young magmatism in Eastern Anatolia. Necioglu (1999) investigated crustal and upper mantle structure between Iran and Turkey by using the Rayleigh wave dispersions. Buyukutku (2003) studied the Miocene carbonate rocks that are accepted as a major reservoir rock within all basins in the eastern part of Turkey.

Gok et al. (2003) used the Sn attenuations in the Anatolian and Iranian Plateau and surrounding regions. Keskin (2003) developed an alternative model for the collision-related volcanism in Eastern Anatolia, and Orgulu et al. (2003) studied the seismotectonics of Eastern Turkey. Sandvol et al. (2003a, b) evaluated the region as a continent–continent collision area, whereas Sengor et al. (2003) interpreted the plateau in Eastern Anatolian as a mantle-supported, domal structure. Angus et al. (2006) proposed a model for the lithospheric structure of eastern Turkey taking place between the Arabian and Eurasian collision zones. Bektas et al. (2007) used the potential field data for the first time and investigated the regional geothermal characterization of East Anatolia, and Gok et al. (2007) investigated the continent–continent collision zone.

The generalized stratigraphic columnar section of the Van Basin is given in Fig. 2 (Buyukutku 2003). The basement is composed of ophiolitic melange and metamorphic rocks of marbles, serpentine, slate, and gneiss. These units are overlain by the Eocene–Oligocene-aged Penek Formation's terrestrial and shallow marine deposits such as

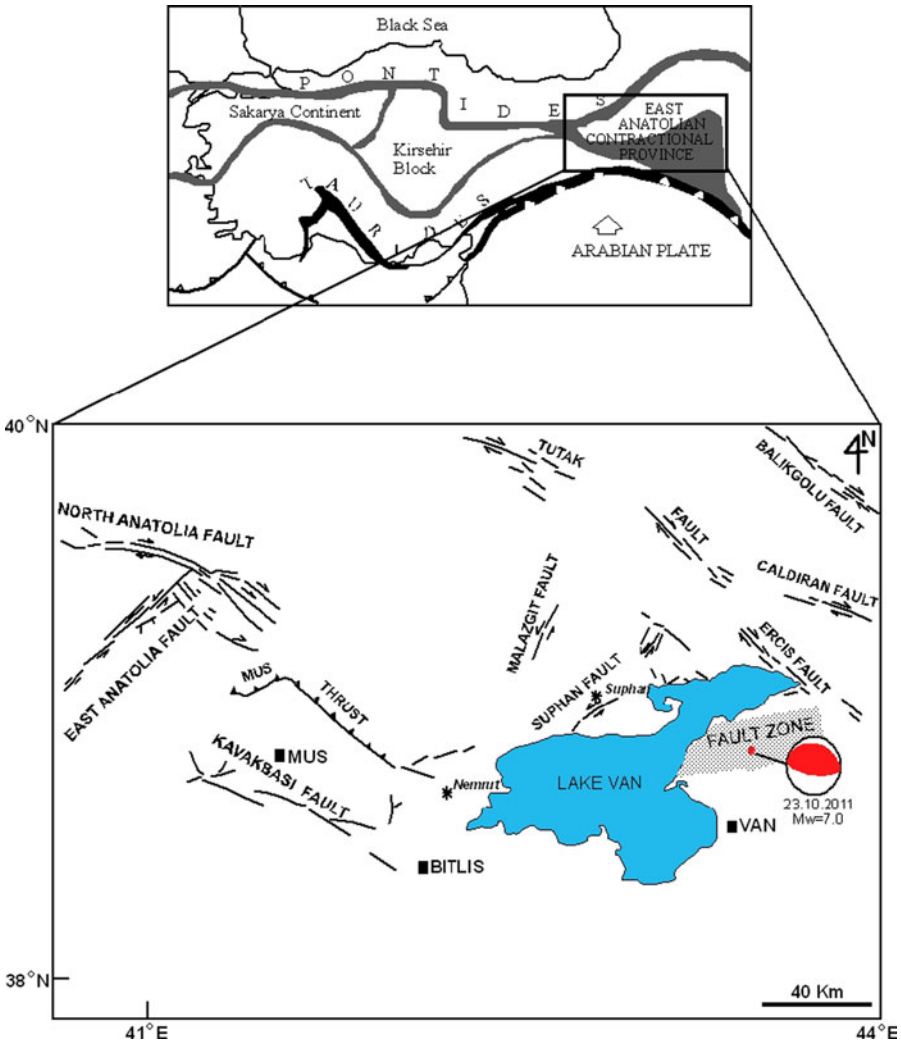

Fig. 1 Active fault map of the study area. Significant faults were taken from Saroglu et al. (1992). The location of the study area is shown by the rectangle in the inset map of Turkey. The location of the main shock that occured on October 23, 2011 is shown by the *solid red circle*. The focal mechanism solution was prepared by the Directory of Disaster and Emergency Management

conglomerates, coarse-grained sandstones, shales, marls, and limestones. The Penek Formation was covered by the Komurlu Formation deposited in a lacustrine–shallow marine environment. This formation is accepted as the Turkish equivalent of the world-class source rock of the Oligo–Miocene Maikopian Formation in the Caspian region. Reefal limestones of the mid-Miocene Adilcevaz Formation above (Buyukutku 2003) are the main reservoir unit for the HC exploration and, together with the Komurlu Formation below and Upper Miocene Zirnak Formation with top seal characteristics above, they constitute a petroleum system. All formations are covered by the Pliocene Karakurt volcanics after an unconformity; these volcanics are sometimes alternated with clastics. When these coarse-

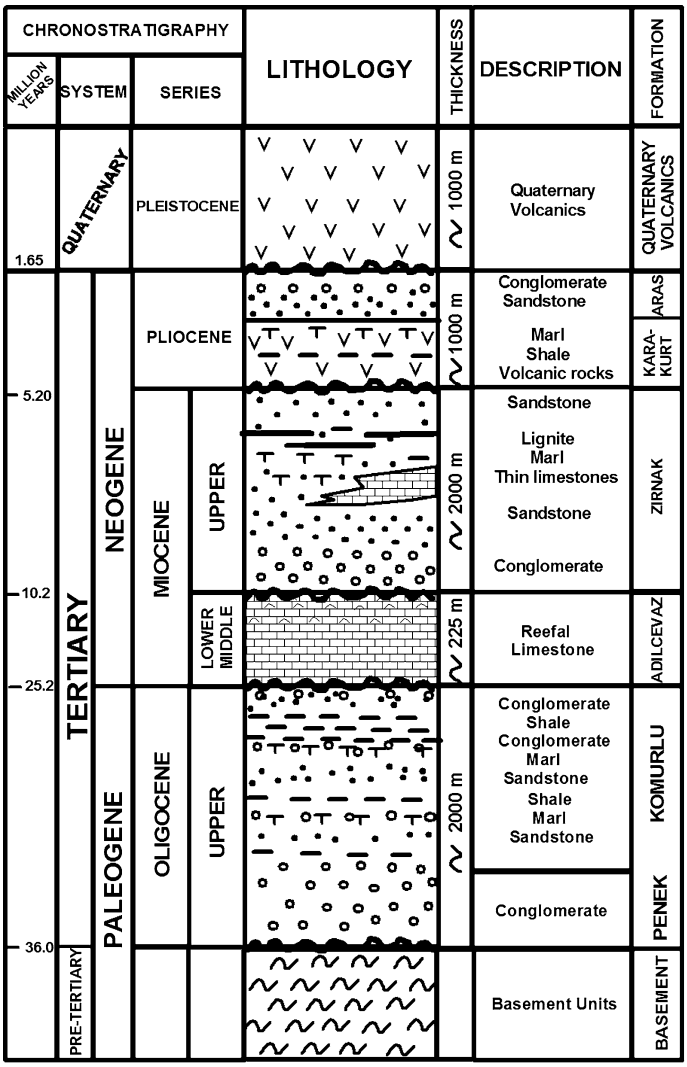

Fig. 2 Generalized stratigraphic columnar section of the Van Basin. Simplified from Buyukutku (2003)

grained clastics are thick enough to form a formation on top of the volcanics, they constitute a new formation and this is called as the Aras Formation. Finally, there is another and younger unnamed Pleistocene volcanic unit at the upper part of the stratigraphic section. The thicknesses of these volcanics are variable, and alluviums around the rivers and tributaries might be thick in some places.

The aim of this paper is to evaluate the deep structure of the basin in the study area using gravity and aeromagnetic data, and to reveal prospective areas for HC and geothermal potential. In addition, it also aims to explain the origin of the volcanics on the surface, to investigate the faults and possible structural elements that may have caused the devastating earthquake that occurred on October 23, 2011. Following this earthquake, several moderate earthquakes occurred as well as aftershock activity in the faulted area.

The fault plane solution indicates that an east–west directional thrust fault caused this earthquake (Fig. 1); it is interesting that the direction of the thrust and other faults in the vicinity is in line with the slightly curved trending anomalous event observed in the aeromagnetic anomalies.

Investigating the hydrocarbon potential of the Van Basin is crucial, because oil production in Anatolia was initially recorded in Kurzot village that is located to the east of Lake Van (Coban 2009). However, HC exploration activities were neglected up to now, and there is only one exploration well (Cakirbey-1) drilled and two seismic lines shot within the Van Basin. Meanwhile, there are more wells drilled in the Mus Basin, and there is much denser seismic coverage to the north and northwest of Lake Van. Because the Mus Basin will be studied, separately, it will only be mentioned briefly in this paper. The seismic quality of two lines in the Van Basin is poor because of the volcanic rocks on the surface (Bayram 2012, personal comm.). As a result of poor seismic quality, the geophysical evaluation in this study was only based on the processing and interpretation of the gravity and aeromagnetic data. However, these data allowed us to determine the location of the depocenters where the sedimentary units including hydrocarbon source rocks may have been deposited. The geographical proximity of these depocenters to Kurzot village and the thickness of the sedimentary rocks in the borehole are proof of the modelling studies in this investigation and HC potential of this region.

2 Gravity and Aeromagnetic Data

The gravity and aeromagnetic data of the region were obtained from the General Directorate of the Mineral Research and Exploration (MTA). Latitude, free air, Bouguer, topographical and tidal corrections were applied by the MTA to the measured gravity data in order to obtain complete Bouguer data. Technical details of both data sets were given in Ates et al. (1999). The gravity anomaly map after all corrections were applied is given in Fig. 3 with 5 mGal contour intervals. Because there is no gravity data collected in the lake, the area covered by the waters of the lake was blanked in all gravity maps. Gravity anomalies are generally represented by negative contours, and broad negative gravity anomalies with closed contours are accepted to represent basins in the region. In order to construct a 3D model of the basin, the gravity anomaly map was limited to cover only the Van Basin that is composed of three different depressions aligned in the N–S direction. The deepest part of the Van Basin is represented by −180 mGal contour closure to the S–SE of Van city center. The depression in the middle covers a relatively smaller area to the NE of Van city center and is represented by −170 mGal contour closure as another deep depression. The basin turns to the NW after the depression in the middle and deepens through the third and the northernmost depression of the basin where the deepest part is also represented by −170 mGal contour. The three depressions are separated from each other by relatively high uplifts or magnetic intrusions. These predictions will be explained in the following sections in detail.

The aeromagnetic data were acquired with 600-m flight altitude, and the total component of geomagnetic field was measured along the N–S trending profiles. Flight lines have generally 1–2 km spacings with the sampling interval of 70 m. After the acquisition, measured values were reduced to the October 1982 base value with daily variation and direction error corrections. The "International Geomagnetic Reference Field-IGRF" values were calculated using a program developed by Baldwin and Langel (1993). The IGRF removed residual aeromagnetic anomaly map is given in Fig. 4 with a contour interval of

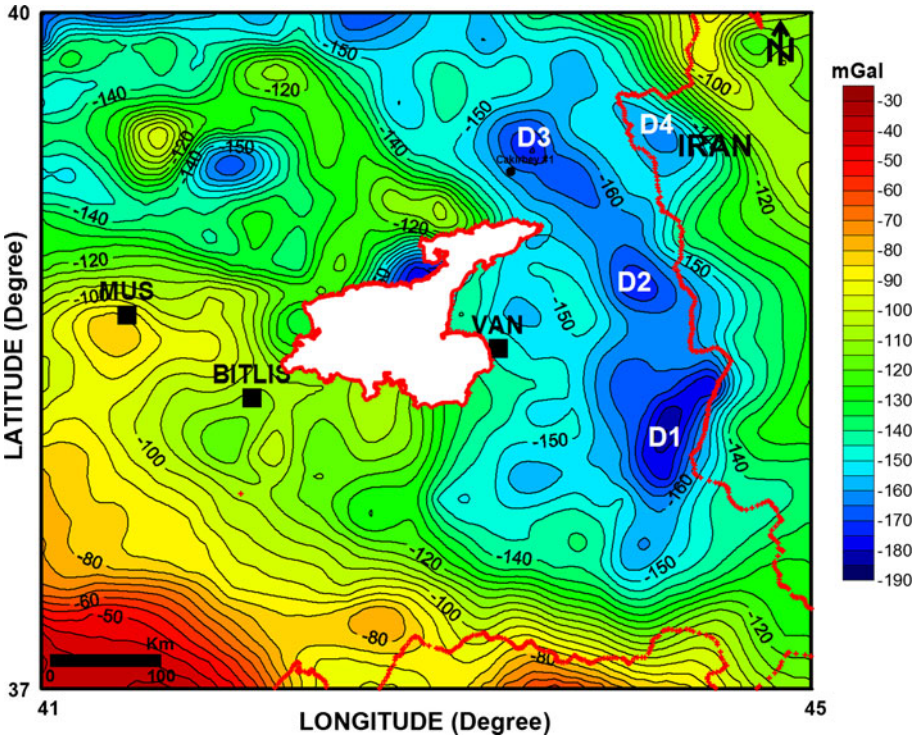

Fig. 3 Gravity anomaly map. Contour interval is 5 mGal. *D1* Depression No. 1, *D2* Depression No. 2, *D3* Depression No. 3, *D4* Depression No. 4

100 nT. Because the data were collected by using an aeroservice, the data were also acquired over the lake in contrast to the lack of gravity data. In this map, the westernmost anomaly coincides with the Nemrut volcanic mountain that is still active with gas seepage in the crater lake on the top of the mountain. From this volcano, there are successive anomalies extending to the east. The second one represents another volcanic mountain named Suphan. Magnetic anomalies are naturally expected to arise from volcanic rocks/activities. However, other magnetic anomalies to the east of Suphan are not represented by volcanic mountains. In this case, they might have been created by buried magmatics. Their lesser intensity and smaller areal coverage in comparison with the anomalies to the west support this idea. Their successive linear elongation within the E and W direction creates the thought that a long fault zone starting from the Nemrut mountain in the west may exist through to the east of Lake Van (Fig. 4). The focal mechanism solution prepared by the Directory of Disaster and Emergency Management (AFAD 2011) for the major earthquake that occurred on October 23, 2011 shows a thrust fault elongated in the east and west direction, supporting the active nature of it (Fig. 1).

There is another large anomaly at the southeastern corner of the lake. It is interesting that this is a single positive polarity anomaly, implying the presence of remanent magnetization. This phenomenon is also valid for some anomalies to the north (Fig. 4).

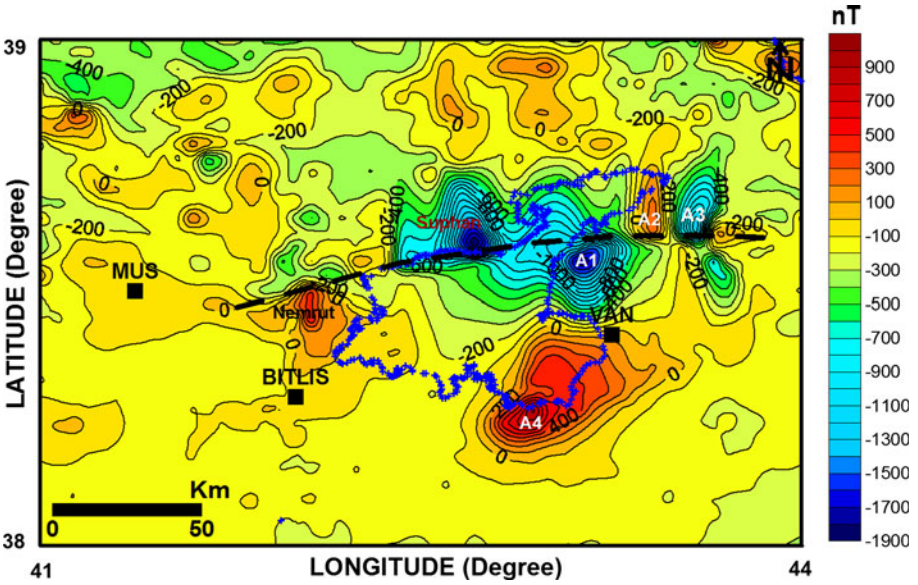

Fig. 4 Residual aeromagnetic anomaly map. Contour interval is 100 nT. *Broken line* in the *center* indicates a possible fault zone. *A1* Anomaly No. 1, *A2* Anomaly No. 2, *A3* Anomaly No. 3, *A4* Anomaly No. 4

3 Well Data

The only hydrocarbon exploration well is the Cakirbey-1 drilled to test the stratigraphy in the Van Basin (Fig. 3). Volcanics were encountered after the initial 6 m, and andesite was dominantly penetrated down to 885 m. After the volcanics, sedimentary rocks belonging to Lower and mid-Miocene times were drilled until 2,115 m and then the basement composed of the ophiolitic melange was encountered. The well was abandoned after approximately 100 m penetration into the basement, and the total depth (TD) was 2,211 m in the melange (Bayram 2012 personnel comm.). The well penetrated 1,230 m thick sedimentary units that are mainly composed of carbonates, marls, and some thin shale bands, indicating a shallow depositional environment. As a result, there is no HC show in this well, and it could not be accepted as a successful stratigraphic test well regarding its location in the Van Basin, either. This result will be emphasized in the following section of 3D modelling.

4 Applied Methods: Upward Continuation, Vertical Derivative, and Analytic Signal

Upward continuation is based on the calculation of the potential field without measuring the actual data on a surface, which is distant from the observation surface. It is used to suppress short wavelength anomalies that are accepted as a high frequency component, or noise interference in long wavelength anomalies of deep sources (Blakely 1996). It may be considered as a kind of filter process to reveal the main structures. It also makes the ambient anomaly much smoother. The mathematical expression of the upward continuation is explained by Gunn (1975).

In this study, the gravity data were upward continued up to 10 km above the ground surface with 1 km steps in order to determine the major depressions in the Van Basin. In a

similar way, the aeromagnetic data were also continued upward to 10 km with 1 km steps. The aim of the upward continuation of the aeromagnetic data is to suppress the effects of the volcanic blanket covering vast areas on the surface and to expose the deep, large intrusions. Another possibility is to determine whether the uplifts between major depressions are created by the magmatic intrusions or whether they are tectonic structures. In hydrocarbon (HC) exploration, tectonic structures or uplifts are prospective areas, but magmatic intrusions (or structures created by the intrusions) should be avoided for drilling and further exploration activities such as shooting a seismic program on these kind of buried structures.

Upward continuation up to 5 km is found to be enough to distinguish shallow and deep structures for both of the gravity and aeromagnetic anomalies. Further upward continuations only make major anomalies much smoother.

The vertical derivative in potential field methods is an application to distinguish the effects of local masses from the ambient, regional field data. The reason for using the derivative may be explained as follows; the effects of local and relatively small masses are often concealed and included in the response of more regional, large masses. First derivative applications are used to differentiate deeper and more regional concealed masses, and to resolve and enhance shallow sources. The vertical derivative of the potential field is performed by the operator given by Gunn (1975).

In this study, the gravity and aeromagnetic anomaly maps were only subjected to the first vertical derivative in order to determine concealed local tectonic highs (structures) between the depressions of the Van Basin. A linear elongation indicating a fault zone from the Nemrut and Suphan mountains through the east was clearly observed in the derivative map. This phenomenon will be explained in the following sections in detail.

Magnetic anomalies are generally represented by a positive (+) or a negative (−) polarity, similar to a magnet. Because of the dipolar nature of a magnetic anomaly, contours representing polarities expand out from the exact location of the causative body. As a result, areal coverage of these bodies cannot be estimated from the aeromagnetic anomaly maps, either. In order to exhibit the elongation and exact location of the causative bodies, the aeromagnetic map was transferred to the analytic signal (AS), which is independent of the magnetization direction (Blakely 1996). AS could be expressed as the sum of the vertical and horizontal gradients of the magnetic anomaly, and it is formulated by Roest et al. (1992).

AS transformation has been used frequently for the accurate interpretation of the potential field data in Turkey such as Bilim (2007, 2011), Aydemir and Ates (2008), Aydemir (2009, 2011), and Demir et al. (2012). In this study, AS transformation was applied only onto the aeromagnetic anomalies, and the slightly curved trend along east–west direction became much clearer. In addition, the exact locations of Nemrut, Suphan, and, more particularly, other buried magmatic intrusions to the east were determined accurately. In the following sections, these regions will be discussed for their inconvenience for the HC exploration strategies.

5 Interpretation of Processed Aeromagnetic Anomaly Maps

There are two important and more evident trends in the aeromagnetic anomaly map of the study area given in Fig. 4. The first one is elongated from the Nemrut mountain at the west side of Lake Van and extending inline through the east of the lake crossing the Suphan mountain. The other one (A4) is located to the southeast corner of Lake Van and to the

southwest of Van city (Fig. 4). The alignment of the anomalies in the north resembles a fault zone. In order to display the linear elongation of the fault, the first derivative of the magnetic anomaly map was prepared. In the first derivative map in Fig. 5, the linear alignment of the fault becomes more evident. As a result of this observation, we can come up with the idea of existence of a fault zone from the Nemrut volcano in the west, following the northern shoulder of the lake and the Suphan volcanic mountain, through the east of the northern throat of the lake. However, this fault zone does not reach to the Turkish and Iranian border. Its eastern end lies between the Turkish national border and the northern throat of the lake. Large magnetic anomalies on this fault zone are most probably created by the volcanics of the Nemrut and Suphan volcanoes, and buried magmatic intrusions to the east of these volcanic mountains because two anomalies to the west could easily be correlated with the Nemrut and Suphan volcanoes (Fig. 5). These correlated anomalies could be accepted as evidence for the magmatic origin of the anomalies (A1–A3) to the east of the Suphan mountain, although these intrusions are not represented by large eruptions as occurred at the Nemrut and Suphan volcanoes. Particularly, the anomaly A1 is more apparent having a similar size to the Suphan anomaly. Other anomalies to the east (A2 and A3) are relatively smaller and their intensities are also less than the anomaly A1. Although these buried volcanic masses are the products of the fault zone mentioned above, they may also have acted as a barrier in the neotectonic time. Because of this, there are many young tectonic features such as thrusts, strike-slip, and normal faults observed in the region to the south of the magnetic anomalies (see Fig. 1.15 in the report of AFAD 2011). This fault zone is represented by a gray belt in Fig. 1.

Another evident, large anomaly (A4) is located to the SW of Van city, and it is represented by only positive contours covering a large area. Its intensity is quite high, and it is composed of only positive polarity. The most critical anomalies in the study area are

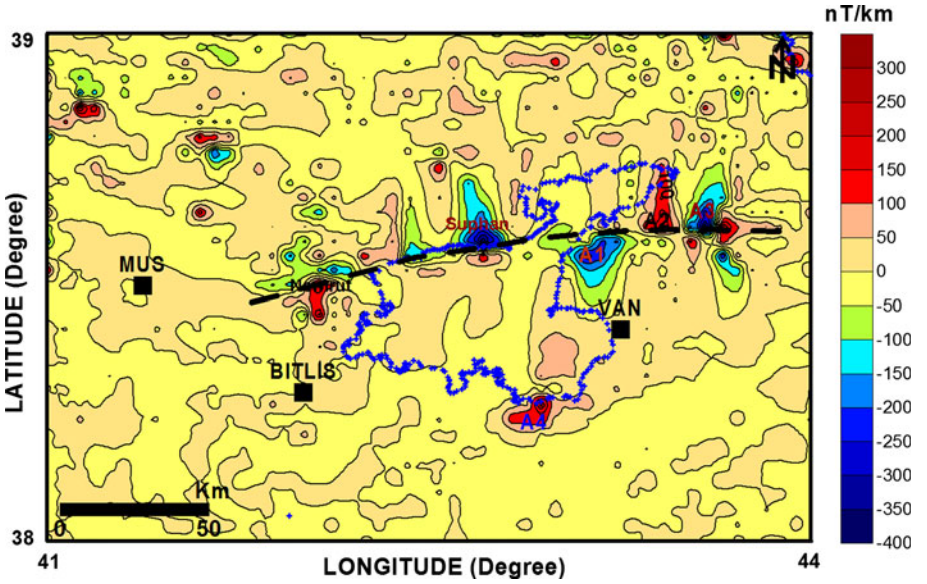

Fig. 5 First vertical derivative map of the magnetic anomalies in the study area. *Broken line* in the center indicates a possible fault zone. *A1* Anomaly No. 1, *A2* Anomaly No. 2, *A3* Anomaly No. 3, *A4* Anomaly No. 4

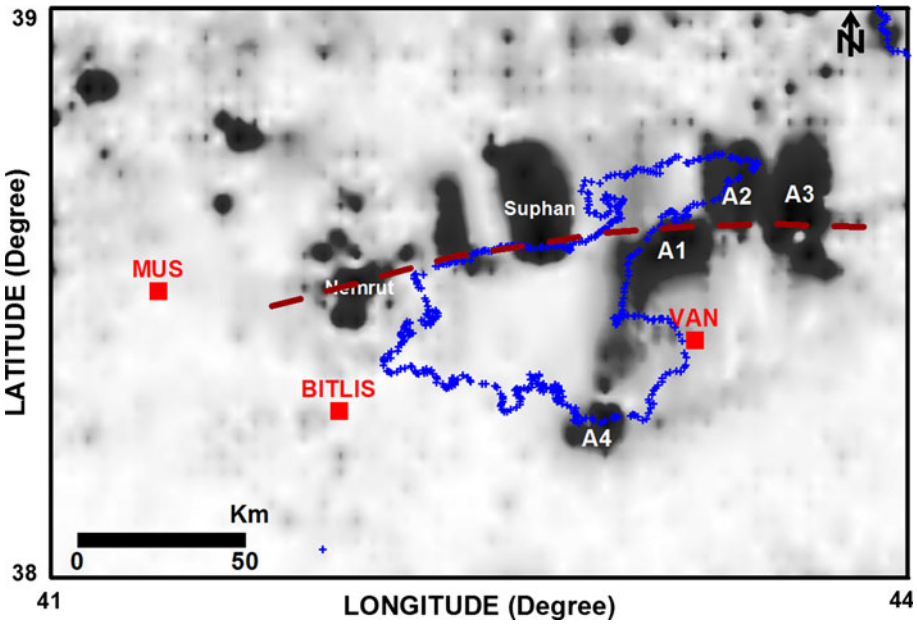

Fig. 6 Analytic signal (AS) map. *Broken line* in the center indicates a possible fault zone. *A1* Anomaly No. 1, *A2* Anomaly No. 2, *A3* Anomaly No. 3, *A4* Anomaly No. 4

the easternmost anomalies (A1–A3) on the fault zone mentioned above because their locations are consistent with the ridge between the depressions in the middle (D2) and to the north (D3). In order to see the exact locations of the causative intrusive bodies, we should refer to the AS map given in Fig. 6. In this map, there are interesting structures. The first one is located between the Nemrut and Suphan mountains; it is quite large and closer to Suphan. Although this causative body is different from Suphan, its effects are combined with the Suphan anomaly and they together create a large anomaly. The resolution of these separate anomalies is almost impossible without the AS map. The other observation is related to the body causing the anomaly A4. In spite of its large anomaly, the areal coverage (size) of the causative body is quite small in comparison with its anomaly. Two causative bodies located nearby to the northeastern extension of the lake are distinguished by their large areas. However, the causative body of the A3 anomaly may be composed of two or three different intrusions close to the each other and they altogether may have created such a large anomaly. Although the AS transformation of the anomalies presents the exact locations of the causative bodies, they do not show whether they are shallow or deep-seated intrusions, or allow any prediction about the thickness and depth of the causative masses. In order to make some assumptions for the depth, it is necessary to apply some processes on the anomalies. The upward continuation is one of the processing methods to distinguish the magnetic anomalies created by the deep-seated causative intrusions from the effects of relatively thin, surficial volcanic cover. In relation with this main concern, the upward continuation up to 10 km from the ground surface with 1 km steps was applied to the aeromagnetic anomaly data. It was observed that widespread anomalies represented by only one contour to the north of the study area were immediately removed and major anomalies started to be smooth, even in the first 1 km upward continuation map. Other anomalies to the east (A1–A3) have no eruption centers, or volcanic

rocks on outcrops may have come to the surface splitting from fractures similar to shield-like volcanism. Because of this, the thickness in general should be less except for low topographical ground levels (valley type). In accordance with this expectation, the thickness of the volcanics penetrated in the Cakirbey-1 well is 876 m (Bayram 2012, personal comm.) where the volcanics are relatively thick.

There is another interesting observation about the eastern anomalies (A2 and A3) that there are two causative bodies at the northeastern extension of the lake in the AS map (Fig. 6); the anomaly A3 keeps its shape in all upward continuation maps, but the A2 is removed and is not presented in the 5 km upward continuation map (Fig. 7) any longer. In this case, the causative body of A2 may be accepted as a major branch of the A3 intrusion that could have a deeper root, and this intrusion may geographically be correlated to the ridge separating the northernmost depression from the other one in the middle. As a result, this region in the subsurface loses its importance and becomes less attractive for HC prospecting.

6 Interpretation of Processed Gravity Anomaly Maps

The Van Basin directly extends parallel to the Turkish and Iranian border in the N–S direction. It turns to the NW from the northern extremity of Lake Van. In addition, the easternmost buried intrusion of magnetic anomaly A3 intersects the ridge between D2 and D3 depressions. There is another interesting observation in the gravity anomaly map that the contours at the eastern and western boundary of the northernmost part of the Van Basin display a dense trend, parallel to the elongation of the basin. This type of contour pattern in gravity maps may indicate the existence of faults. Hence, the right lateral strike-slip Tutak Fault and following Ercis Fault to the south can be observed in the "Turkish Active Faults

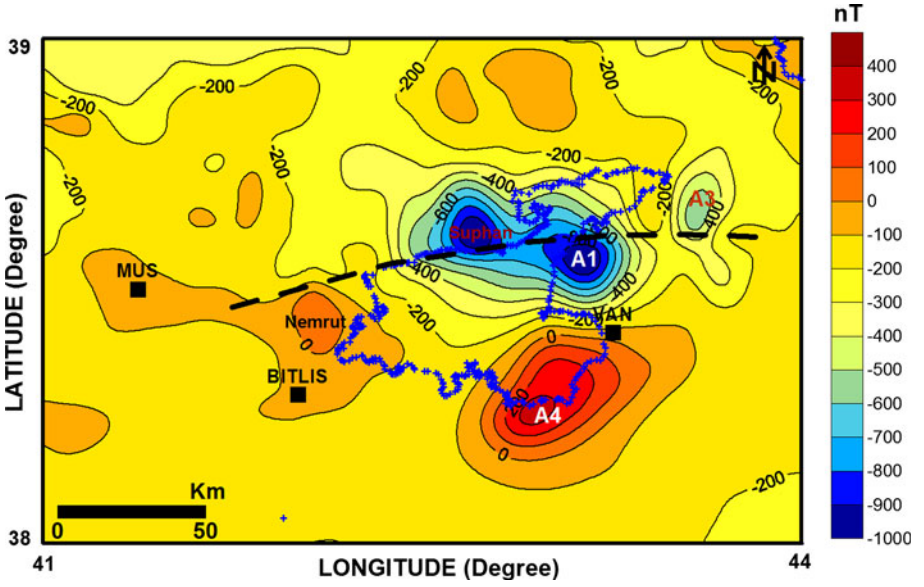

Fig. 7 Aeromagnetic anomalies after 5 km upward continuation. Contour interval: 100 nT. *A1* Anomaly No. 1, *A2* Anomaly No. 2, *A3* Anomaly No. 3, *A4* Anomaly No. 4

Map" (Fig. 1) modified from Saroglu et al. (1992) where there are frequent parallel contours at the western margin of the northwestern depression (D3) of the Van Basin. Similarly, the right lateral Balikgolu Fault extends in the eastern margin of the same depression where the contour pattern becomes denser.

The deepest part of the basin (D1) should be the southern part because contour values are represented as low as −180 mGal (Fig. 3). After an increase in the contour values to the north, the depression in the middle (D2) is located to the E–NE of Van city and it is represented by −170 mGal contour as the lowest value (Fig. 3). The uplift between the southern (D1) and the second depression in the middle (D2) could be the initial exploration area. There must be another ridge that could have been formed by the buried magmatic intrusion of anomaly A3 as explained above in between the northern depression (D3) and the depression in the middle (D2). The basin deepens to the northwest with the −170 mGal contours as again the lowest values. The northern part of the basin is totally covered by young volcanic flow. Therefore, it is not easy to predict the existence of such a basinal depression beneath the volcanic cover from the surface observations. There is another depression area related with the Van Basin to the northeast, but it is located at the Iranian border (D4). There is a subsurface ridge between these two northerly depressions (D3 and D4), and this area could be a promising prospective area for HC exploration because there is no magnetic anomaly correlated to this region. It may be a tectonic uplift or a basement ridge. In case of its being a shallow structure, its prospectivity for HC production may decrease significantly.

In addition to structures between the deeper parts of the basin, undulations and prospects (if there are any) right in the middle of depressions are worthy of being given priority because they are located directly in the "kitchen area" where they could be filled with hydrocarbons expelled from in situ source rocks deposited in the Van Basin. In order to expose and distinguish anomalies of the prospective local structures from the effects of the ambient depressions, the first vertical derivative was also applied to the gravity data. The first vertical derivative map of the study area is given in Fig. 8. According to this map, the northwestern depression (D3) is composed of two different contour closures. The area between the closures could be a prospective zone, and it is accompanied by another closure, close to the area in the middle. A similar phenomenon is valid for the southern depression (D1) as well. Moreover, the northern closure of this depression has three different sub-closures, and there are many small closures to the west of the depression D1. All these closures could be prospective being away from the magnetic anomalies. However, these structures are smaller than the ridges located between the depressions. Particularly, the basement high between the southern depression (D1) and the depression in the middle (D2), and the tectonic high between the northwestern depression (D3) and the depression in the Iranian border to the north (D4) are important and attractive for HC exploration. The latter is composed of two different closures, but it should be treated as a single structure in general. The northern part of the Van Basin is close to the major magmatic intrusions and volcanic eruption center of the Suphan mountain. These volcanic activities do not have a direct influence on HC generation, but they may make a positive contribution to the maturation of the HCs generated.

In order to determine how deep or shallow these depressions are, the gravity data were also upward continued as was done for the aeromagnetic data. In the first 1 km upward continuation, there is not any significant change in the contour patterns except smoothing. However, in the 2 km upward continuation map (Fig. 9), the northern depression in Iran (D4) and the depression in the middle (D2) are both characterized by only one contour. Additionally, closures next to the north of Van city and to the SE of Lake Van in the

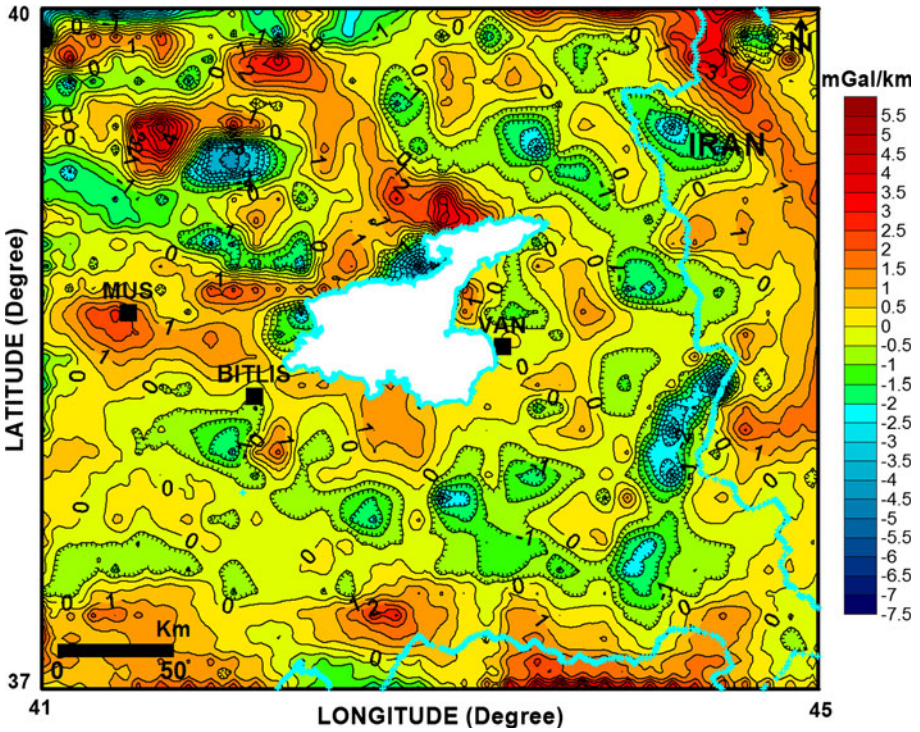

Fig. 8 First vertical derivative map of the gravity anomalies in the study area

gravity anomaly map (Fig. 3) are removed. Therefore, they may be accepted as small and shallow depressions. The northeastern depression in Iran (D4) is totally removed in the 5 km upward continuation map (Fig. 10). However, it should be deep enough for HC generation. From this point of view, the uplift to the west of the depression D4 deserves further exploration activities. Since the other upward continuation maps display only contour smoothing, they will not be given in this paper. All three major depressions of the Van Basin are permanent in all upward continuation maps up to 10 km.

7 Three-Dimensional (3D) Modelling of the Van Basin

Priority was given to 3D modelling of the Van Basin in order to determine how deep those depressions are; the 3D modelling is based on the method of Cordell and Henderson (1968). In general, the 3D iterative modelling might be calculated for the causative body assumed to be flat topped or flat bottomed. Because the basins are syncline shaped, the model was constructed according to the flat top assumption. The density contrast is the most important parameter for the construction of models.

The densities to be used for the calculation of the density contrast between the basement and sedimentary units were obtained from the literature (Telford et al. 1990). The sedimentary basin fill is mainly composed of low-density units, dominantly shales and sandstones with densities changing between 2.35 and 2.40 Mg m^{-3}. Thus, an average of 2.38 Mg m^{-3} can be accepted as a descriptive value for the sedimentary basin fill. The

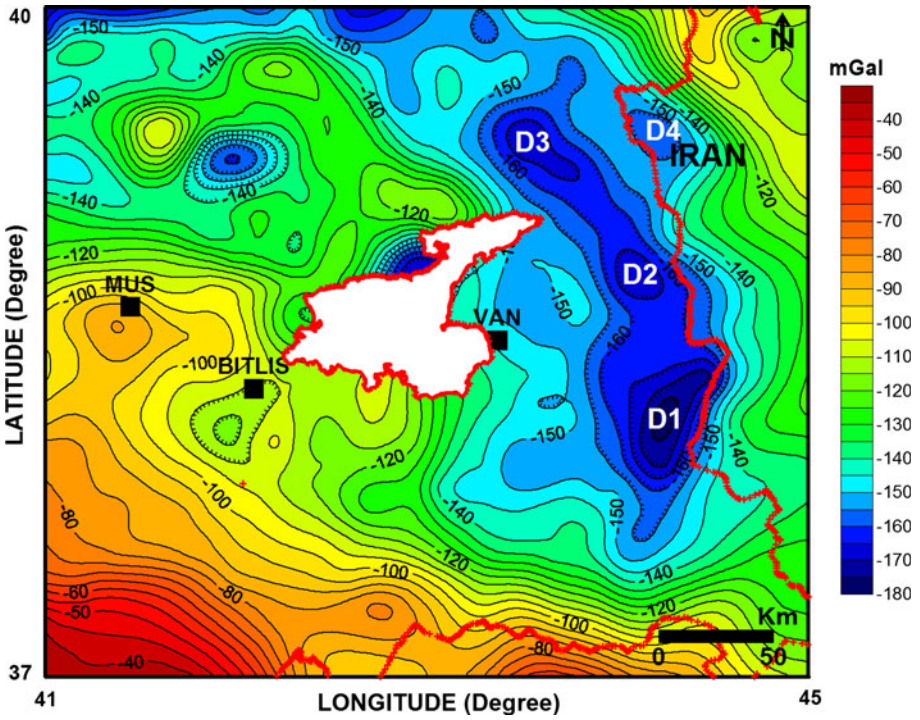

Fig. 9 Gravity anomalies after 2 km upward continuation. Contour interval: 5 mGal. *D1* Depression No. 1, *D2* Depression No. 2, *D3* Depression No. 3, *D4* Depression No. 4

basement is composed of marbles, serpentine, slate, and gneiss. The densities of these metamorphic units were taken as 2.75–2.80 Mg m^{-3} from Telford et al. (1990). Because the widespread intrusions of igneous rocks are important and they form the basement for the sedimentary units around the northern and central depressions, their contribution should also be considered to determine the density contrast. When Telford et al. (1990) is referred to again, the average density of the basic igneous rocks is found to be 2.79 Mg m^{-3}. Altogether with the igneous rocks and metamorphics, the average density of the basement can be taken as 2.78 Mg m^{-3}.

In this case, a density contrast of −0.4 Mg m^{-3} should be used for the construction of the 3D model. Figure 11a, b display the 3D model map prepared according to this density contrast of −0.4 Mg m^{-3}. In this map, all depressions deepen sharply, particularly the northern depression (D3) and the depression in the middle (D2) show immediate, circular deepening, but the geometry of depression to the south (D1) is oval and it is composed of two sub-depressions. The maximum depth in the northern depression (D3) is around 8 km while it is 6 km for the depression in the middle (D2). The maximum depth extends down to 15 km in both of the sub-depressions to the south (D1). The areal extension of depression D1 is larger than the other depressions to the north (D2 and D3), and it is more convenient for the HC generation in comparison with the others in case of having source rock deposition. Meanwhile, the ridges separating all depressions from each other are shallow, around 1–1.5 km.

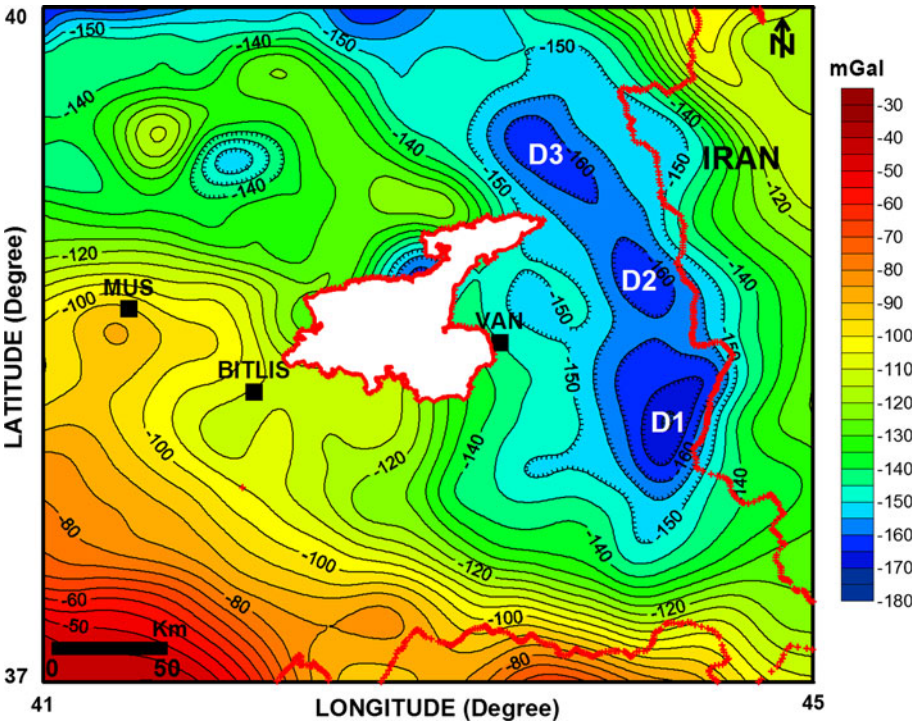

Fig. 10 Gravity anomalies after 5 km upward continuation. Contour interval: 5 mGal. *D1* Depression No. 1, *D2* Depression No. 2, *D3* Depression No. 3

8 Discussion and Conclusions

The study area includes almost all the southeastern and eastern part of Turkey around Lake Van. In this study, the deep structure of this area was investigated first by using gravity and aeromagnetic data. The NAF is observed toward the 40 km northwest of Lake Van from the active tectonic map given in Fig. 1. It may be confirmed from the gravity anomalies that the intensifying trend of contours extends from this position toward Lake Van in the northwesterly direction. Aeromagnetic anomalies (Fig. 4) and the processed products of them such as the vertical derivative and AS maps show a slightly curved east–west trending lineament. The focal mechanism solution of the major event of October 23, 2011 shows an earthquake caused by a thrust fault elongated in the same direction, and it is well correlated with this lineament. Because the area is intensively faulted, after the main event, several moderate earthquakes occurred such as the earthquake on the November 9, 2011 with a magnitude of 5.6 that was felt strongly because of its proximity to Van city. Later, the study was focused onto the Van Basin for its HC potential, which is located to the east of the largest lake in the country. The earliest oil production was recorded in this region (around Kurzot village) with primitive methods (gravitational fill out of the pools from the seepages) before the foundation of the Turkish Republic. However, this area has been neglected regarding HC exploration using modern techniques. There are only two, poor-quality seismic lines shot and only one exploration well, Cakirbey-1, drilled in the region

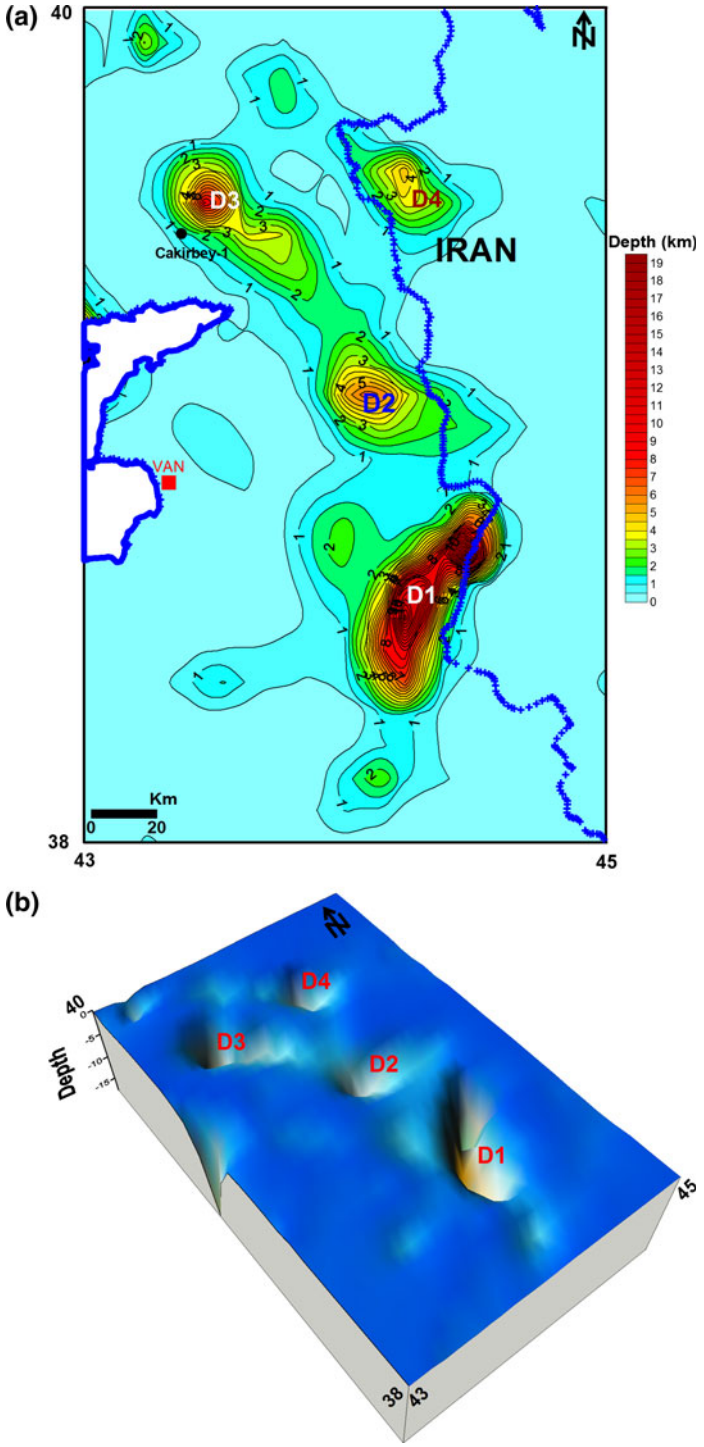
(a)
40
38
43
45
N
D1
D2
D3
D4
IRAN
Cakirbey-1
VAN
Km
0
20
Depth (km)
19
18
17
16
15
14
13
12
11
10
9
8
7
6
5
4
3
2
1
0
(b)
N
D1
D2
D3
D4
Depth
40
38
43
45

◀ **Fig. 11** **a** Three-dimensional (3D) depth model map. Contour interval: 0.5 km. *D1* Depression No. 1, *D2* Depression No. 2, *D3* Depression No. 3, *D4* Depression No. 4. **b** Three-dimensional (3D) model surface map. *D1* Depression No. 1, *D2* Depression No. 2, *D3* Depression No. 3, *D4* Depression No. 4

(with no HC shows). As a result, only surface geological observations and gravity and aeromagnetic data are available in the study area.

According to the gravity anomaly map (Fig. 3), the Van Basin is composed of three different, narrow and long depressions. The southern depression (D1) is the deepest one. There are some dorsal ridges separating these depressions from each other. These uplifts could be good prospective regions, except for the structure between the northern depression (D3) and the depression in the middle (D2). There is a fault zone from the Nemrut mountain to the west, extending through the east of the lake crossing the Suphan mountain. Volcanic eruptions from those mountains and magmatic intrusions represented by magnetic anomalies to the east are all arranged along the course of the slightly curved fault zone. The easternmost of these anomalies could be correlated to the ridge between the mid- (D2) and northern depressions (D3) mitigating the HC prospectivity of this area. However, it may have positive influences on the maturity of the source rocks within the basin.

The contour lines on the margins of the depression D3 are dense and parallel to each other in the gravity anomaly map. This made us think that the northern margins of the Van Basin may be fault controlled from the east and west by the Balikgolu and Tutak-Ercis Faults, respectively. These margins (particularly the eastern margin) could be good for prospecting because this zone is surrounded by two depressions (D3 and D4). In addition, there are relatively high structures in the southern (D1) and northern (D3) depressions dividing each of them into two sub-depressions. They are located between the deepest closures and have a chance of being filled by HCs directly from the "kitchen area." Furthermore, they are under the conditions of temperature and overburden pressure as required for HC generation and maturation.

Acknowledgments The authors are grateful to the General Directorate of Mining Research and Exploration (MTA) of Turkey for the provision of aeromagnetic and gravity data that were used for a Turkish Scientific Research Council (TUBITAK) project. We thank two anonymous reviewers and the Chief Editor Prof. Rycroft for their constructive critiques.

References

AFAD (2011) Van Depremi Raporu, 23 Ekim 2011. Deprem Dairesi Başkanlığı, Ankara (in Turkish). http://www.deprem.gov.tr/sarbis/Shared/WebBelge.aspx?param=105

Angus DA, Wilson DC, Sandvol E, Ni JF (2006) Lithospheric structure of the Arabian and Eurasian collision zone in eastern Turkey from S-wave receiver functions. Geophys J Int 166:1335–1346

Ates A, Kearey P, Tufan S (1999) New gravity and magnetic anomaly maps of Turkey. Geophys J Int 136:499–502

Aydemir A (2009) Tectonic investigation of central Anatolia, Turkey using geophysical data. J Appl Geophys 68:321–334

Aydemir A (2011) An integrated geophysical investigation of Haymana Basin and hydrocarbon prospective Kirkkavak Formation in Central Anatolia, Turkey. Petrol Geosci 17:91–100

Aydemir A, Ates A (2008) Determination of hydrocarbon prospective areas in the Tuzgolu (Saltlake) Basin, central Anatolia, by using geophysical data. J Pet Sci Eng 62:36–44

Baldwin RT, Langel R (1993) Tables and maps of the DGRF 1985 and IGRF 1990, International Union of Geodesy and Geophysics Association of Geomagnetism and Aeronomy. IAGA Bull 54:158

Bektas O, Ravat D, Buyuksarac A, Bilim F, Ates A (2007) Regional geothermal characterization of East Anatolia from aeromagnetic, heat flow and gravity data. Pure Appl Geophys 164:975–998

Bilim F (2007) Investigations into the tectonic lineaments and thermal structure of Kutahya–Denizli region, western Anatolia, from using aeromagnetic, gravity and seismological data. Phys Earth Planet Inter 165:135–146
Bilim F (2011) Investigation of the Galatian volcanic complex in the northern central Turkey using potential field data. Phys Earth Planet Inter 185:36–43
Blakely RJ (1996) Potential theory in gravity and magnetic applications. Cambridge University Press, UK
Buyukutku AG (2003) The reservoir potential of Miocene carbonate rocks in the Askale and Hinis-Mus-Van sub-basins, East Anatolia, Turkey. J Petrol Geol 26:175–188
Coban MK (2009) Dunden bu gune Turkiye Cumhuriyeti'nde petrol aramalari. Ankara, Turkey
Cordell L, Henderson RG (1968) Iterative three-dimensional solution of gravity anomaly data using a digital computer. Geophysics 33:596–601
Demir D, Bilim F, Aydemir A, Ates A (2012) Modelling of Thrace Basin, NW Turkey using gravity and magnetic anomalies with control of seismic and borehole data. J Pet Sci Eng 86–87:44–53
Gok R, Sandvol E, Turkelli N, Seber D, Barazangi M (2003) Sn attenuation in the Anatolian and Iranian Plateau and surrounding regions. Geophys Res Lett 30(24):8042. doi:10.1029/2003GL018020
Gok R, Pasyanos ME, Zor E (2007) Lithospheric structure of the continent–continent collision zone: eastern Turkey. Geophys J Int 169:1079–1088
Gunn PJ (1975) Linear transformations of gravity and magnetic fields. Geophys Prospect 23:300–312
Jackson J, McKenzie D (1984) Active tectonics of the Alpine-Himalayan Belt between western Turkey and Pakistan. Geophys J R Astr Soc 77:185–264
Keskin M (2003) Magma generation by slab steepening and breakoff beneath a subduction-accretion complex: an alternative model for collision-related volcanism in Eastern Anatolia. Geophys Res Lett 30:8046. doi:10.1029/2003GL018019
Kurtman F, Akkus MF (1971) Dogu Anadolu'daki ara basenler ve bunlarin petrol olanaklari. Bull Miner Res Explor 77:1–9
Necioglu A (1999) Determination of crustal and upper mantle structure between Iran and Turkey from the dispersion of rayleigh waves. J Balkan Geophys Soc 2:139–150
Orgulu G, Aktar M, Türkelli N, Sandvol E, Barazangi M (2003) Contribution to the seismotectonics of Eastern Turkey from moderate and small size events. Geophys Res Lett 30(24):8040. doi:10.1029/2003GL018258
Roest WR, Verhoef J, Pilkington M (1992) Magnetic interpretation using the 3-D analytic signal. Geophysics 57:116–125
Sandvol E, Turkelli N, Barazangi M (2003a) The Eastern Turkey seismic experiment: the study of a young continent–continent collision. Geophys Res Lett 30(24):8038. doi:10.1029/2003GL018912
Sandvol E, Turkelli N, Zor E, Gok R, Bekler T, Gurbuz C, Seber D, Barazangi M (2003b) Shear wave splitting in a group continent–continent collision: an example from Eastern Turkey. Geophys Res Lett 30(24):8041. doi:10.1029/2003GL017390
Saroglu F, Yilmaz Y (1986) Geological evolution and basin models during the neotectonic episode in Eastern Anatolia. Bull Miner Res Explor 107:61–83
Saroglu F, Emre O, Kuscu I (1992) Turkiye Diri Fay Haritasi. MTA Gen. Mudurlugu Yayini, Ankara
Sengor AMC, Kidd WSF (1979) Post collisional tectonics of the Turkish—Iranian plateau and comparison with Tibet. Tectonophysics 55:361–376
Sengor AMC, Yilmaz Y (1981) Tethyan evolution of Turkey: a plate tectonic approach. Tectonophysics 75:181–241
Sengor AMC, Ozeren S, Zor E, Genc T (2003) East Anatolian high plateau as a mantle-supported, north-south shortened domal structure. Geophys Res Lett 30(24):8045. doi:10.1029/2003GL017858
Telford WM, Geldart LP, Sheriff RE (1990) Applied geophysics, 2nd edn. Cambridge University Press, Cambridge
Yilmaz Y, Saroglu F, Guner Y (1987) Initiation of neomagmatism in East Anatolia. Tectonophysics 134:177–199